Letter

Topological terms on topological defects: A quantum Monte Carlo study

Toshihiro Sato,[1] Martin Hohenadler,[1] Tarun Grover,[2] John McGreevy,[2] and Fakher F. Assaad[1,3]
[1]*Institut für Theoretische Physik und Astrophysik, Universität Würzburg, 97074 Würzburg, Germany*
[2]*Department of Physics, University of California at San Diego, La Jolla, California 92093, USA*
[3]*Würzburg-Dresden Cluster of Excellence ct.qmat, Am Hubland, 97074 Würzburg, Germany*

(Received 28 October 2020; revised 23 September 2021; accepted 23 September 2021; published 6 October 2021)

Dirac fermions in $(2+1)$ dimensions with dynamically generated anticommuting SO(3) antiferromagnetic and Z_2 Kekulé valence-bond solid (KVBS) masses map onto a field theory with a topological θ term. This term provides a mechanism for continuous phase transitions between different symmetry-broken states: topological defects of one phase carry the charge of the other and proliferate at the transition. The θ term implies that a domain wall of the Z_2 KVBS order parameter harbors a spin-1/2 Heisenberg chain, as described by a $(1+1)$-dimensional SO(3) nonlinear sigma model with θ term at $\theta = \pi$. Using pinning fields to stabilize the domain wall, we show that our auxiliary-field quantum Monte Carlo simulations indeed support the emergence of a spin-1/2 chain at the Z_2 topological defect. Surprisingly, the consequences of the topological term are seen *far* from the critical point such that the physics of apparently unrelated model systems are naturally understood by invoking them. This concept can be generalized to higher dimensions where $(2+1)$-dimensional SO(4) or SO(5) theories with topological terms are realized at a domain wall.

DOI: 10.1103/PhysRevB.104.L161105

Introduction. Topological terms in field theories play an important role in our understanding of phases and critical phenomena. For instance, the differences between integer and half-integer spin-S chains are a consequence of the $2\pi iS$ prefactor of the integer-valued θ term that counts the winding of a unit vector over the sphere. Dirac fermions provide a very appealing route to define models that map onto field theories with topological terms [1–9]. Consider eight-flavored Dirac fermions in $(2+1)$ dimensions akin to graphene. In this case, there is a maximum of five anticommuting mass terms that could, for instance, correspond to an antiferromagnet (AFM) with three mass terms and a Kekulé valence-bond solid (KVBS) with two mass terms [10]. The ten commutators of these mass terms correspond to the generators of the SO(5) group so that Dirac fermions that are Yukawa coupled to these five mass terms possess an SO(5) symmetry. In the massive phase, one can integrate out the fermions to obtain a Wess-Zumino-Witten (WZW) topological term [1,2] that is believed to be at the origin of deconfined quantum criticality [11,12]. In particular, it formalizes the Levin-Senthil picture [13] of a vortex of the Kekulé order harboring an emergent spin-1/2 degree of freedom.

The aim of this Letter is to demonstrate numerically the consequences of topological terms in the corresponding field theory. We will do so by considering a model of Dirac fermions in $(2+1)$ dimensions with reduced spatial symmetries such that the three AFM and one of the two KVBS mass terms are dynamically generated. Contrary to the generic KVBS state with a spontaneously broken U(1) symmetry in the continuum, our KVBS state spontaneously breaks a Z_2 symmetry. We will refer to this state as Z_2 KVBS. Starting from the WZW topological term, this symmetry reduction amounts to setting one component of the five-dimensional field to zero. This maps the WZW term to a θ term at $\theta = \pi$ [3]. Let us assume that the phase transition observed numerically between the AFM and the Z_2 KVBS is continuous and captured by the aforementioned field theory. Then, the θ term leads to the prediction that in the Z_2 KVBS phase *close* to the transition, a Z_2 KVBS domain wall harbors a spin-1/2 chain. In what follows, we will provide a model—amenable to large-scale negative-sign-free auxiliary-field quantum Monte Carlo (QMC) calculations—that provides compelling results supporting this field-theory picture. The consequences of topology are seen far from the critical point such that surprising results on seemingly unrelated model systems become transparent.

Field theory. A theory that accounts for the phase diagram presented in Ref. [6] [see Fig. 1(a)] contains Dirac fermions that are Yukawa coupled to the AFM and Z_2 KVBS mass terms, as described by

$$\mathcal{L}_{\mathrm{F}} = \Psi^{\dagger}\left[\partial_{\mu}(\mathbf{1}_2 \otimes \gamma_0\gamma_{\mu}) + \begin{pmatrix}\eta_{\alpha}\\ \chi\end{pmatrix} \cdot \begin{pmatrix}\sigma_{\alpha}\otimes\gamma_0\\ \mathbf{1}_2\otimes i\gamma_0\gamma_5\end{pmatrix}\right]\Psi \ . \quad (1)$$

Here, the Dirac spinors $\Psi^{\dagger}$ carry a sublattice index, a spin index, and a valley index. The γ matrices act on the valley and sublattice spaces and satisfy the Clifford algebra $\{\gamma_a, \gamma_b\} = 2\delta_{ab}$. σ_{α} with $\alpha = 1, 2, 3$ denote the Pauli spin-1/2 matrices. The fact that the SO(3) AFM mass terms $\sigma_{\alpha}\otimes\gamma_0$ and Z_2 KVBS mass terms $\mathbf{1}_2 \otimes i\gamma_0\gamma_5$ anticommute results in an SO(4) invariance of the fermionic action: a global SO(4) rotation of the four-component field $\boldsymbol{\phi} = (\phi_1, \phi_2, \phi_3, \phi_4) = (\boldsymbol{\eta}, \chi)$ is equivalent to a canonical transformation of the fermion operators. The dynamics of the field is governed by a

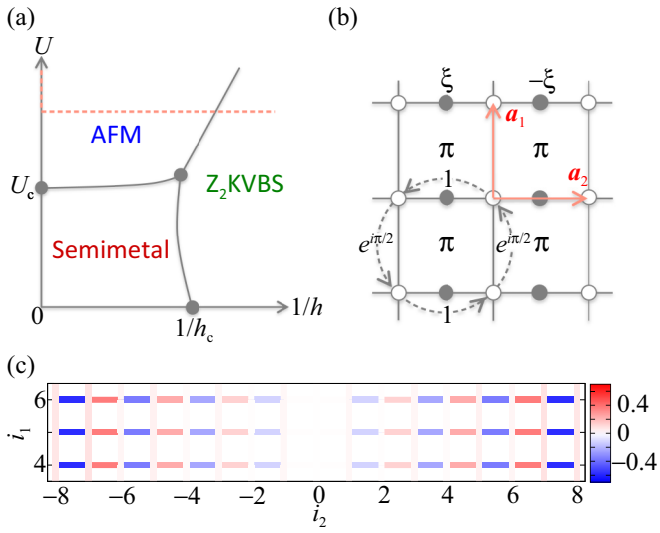

FIG. 1. (a) Schematic ground-state phase diagram [6]. Dashed line indicates scans considered here. (b) In our model, fermions acquire a π-flux when circulating around a plaquette and are coupled to Ising spins on lattice bonds with magnitude $\pm\xi$. We consider periodic (open) boundary conditions in the $\boldsymbol{a}_1$ ($\boldsymbol{a}_2$) directions and freeze the Ising spins on the open boundary to impose the domain wall. (c) Real-space bond energy change, $\Delta\hat{B}_{i,a_l}$. Here, $L_1 = 30$ and $L_2 = 17$.

four-component φ^4 action, $\mathcal{L}_\mathrm{B}$. While $\mathcal{L}_\mathrm{F}$ has SO(4) symmetry, $\mathcal{L}_\mathrm{B}$ inherits the SO(3) $\times$ Z_2 symmetry of the lattice model.

The Lagrangian $\mathcal{L} = \mathcal{L}_\mathrm{F} + \mathcal{L}_\mathrm{B}$ can account for many phase transitions. The Gross-Neveu transitions from semimetal to AFM or from semimetal to Z_2 KVBS involve a closing of the mass gap corresponding to the norm of the field $\boldsymbol{\phi}$. On the other hand, QMC simulations (see Ref. [6] and the Supplemental Material (SM) [14]) point to a continuous transition between the AFM and Z_2 KVBS states with an emergent SO(4) symmetry. Importantly, the numerical results show that the single-particle gap remains finite across the transition. In the field theory, this implies that amplitude fluctuations of $\boldsymbol{\phi}$ are frozen and only phase fluctuations of the field need to be retained. Since the fermions remain massive, they can be integrated out (in the large mass limit) to obtain

$$S = \int dx^2 d\tau \frac{1}{g}(\partial_u \hat{\boldsymbol{\phi}})^2 + i\theta\mathcal{Q}, \quad \theta = \pi, \tag{2}$$

with

$$\mathcal{Q} = \frac{1}{12\pi^2}\int dx^2 d\tau \epsilon_{i,j,k}\epsilon_{\alpha,\beta,\gamma,\delta}\hat{\phi}_\alpha \partial_i\hat{\phi}_\beta \partial_j\hat{\phi}_\gamma \partial_k\hat{\phi}_\delta. \tag{3}$$

Here, $\hat{\boldsymbol{\phi}}(\boldsymbol{x},\tau) = \boldsymbol{\phi}/|\boldsymbol{\phi}|$ defines a mapping from $(2+1)$-dimensional Euclidean space-time to the three-dimensional sphere S^3. For smooth $\hat{\boldsymbol{\phi}}(\boldsymbol{x},\tau)$'s, $\mathcal{Q}$ is quantized and counts the winding of the unit four-vector $\hat{\boldsymbol{\phi}}$ on S^3.

A domain wall of the Z_2 KVBS order parameter is obtained by pinning the field $\hat{\boldsymbol{\phi}}$ at the origin and at infinity: $\hat{\boldsymbol{\phi}}(\boldsymbol{0}) = (0,0,0,1)$ and $\hat{\boldsymbol{\phi}}(\infty) = (0,0,0,-1)$. Let us parametrize $(2+1)$-dimensional Euclidean space-time with spherical coordinates, $(\boldsymbol{x},\tau) = r\boldsymbol{n}$ with $\boldsymbol{n}$ a unit vector, and choose

$$\hat{\phi}(r\boldsymbol{n}) = \{\sin[f(r)]\boldsymbol{n}, \cos[f(r)]\}. \tag{4}$$

Here, f is a one-to-one smooth function with boundary conditions $f(0) = 0$ and $f(\infty) = \pi$ and describes the profile of the domain wall. As shown in the SM [14], the integration over r can now be carried out to obtain the domain-wall action,

$$S_\mathrm{DW} = \int dx d\tau \frac{1}{g}(\partial_u \boldsymbol{n})^2 + i\pi\mathcal{Q}_\mathrm{DW}(\boldsymbol{n}), \tag{5}$$

with

$$\mathcal{Q}_\mathrm{DW}(\boldsymbol{n}) = \frac{1}{4\pi}\int dx d\tau \boldsymbol{n}\cdot\partial_\tau\boldsymbol{n}\times\partial_x\boldsymbol{n}. \tag{6}$$

Above we have mapped S^2 (on which $\boldsymbol{n}$ is defined) to $\mathbb{R}^2$. While the topological term is independent of the choice of the profile of the domain wall, g depends on f. The action in Eq. (5) corresponds to that of the spin-1/2 Heisenberg chain [21,22].

Model. The QMC simulations presented in Ref. [6] for the honeycomb lattice support a direct and continuous transition between the AFM and Z_2 KVBS with an emergent SO(4) symmetry and, in principle, provide a case to test the above predictions. However, irrespective of how one places the pinning fields on the honeycomb lattice, translation symmetry along the domain wall will be broken. Since gaplessness of the spin-1/2 chain is protected by a mixed anomaly between translations and time-reversal or spin rotations, dimerization along the domain wall will occur. Hence, even if a spin chain emerges at the domain wall, it will gap out due to the choice of lattice discretization. To avoid this, we have reformulated the model of Ref. [6] on the π-flux square lattice. This provides a lattice discretization of Dirac fermions with a C_4 symmetry. The model Hamiltonian reads $\hat{H} = \hat{H}_\mathrm{f} + \hat{H}_\mathrm{s} + \hat{H}_\mathrm{fs}$ [see Fig. 1(b)] with

$$\hat{H}_\mathrm{f} = \sum_{\langle ij\rangle,\sigma} t_{ij}\hat{c}^\dagger_{i\sigma}\hat{c}_{j\sigma} + U\sum_i \left(\hat{n}_{i\uparrow} - \tfrac{1}{2}\right)\left(\hat{n}_{i\downarrow} - \tfrac{1}{2}\right),$$
$$\hat{H}_\mathrm{s} = J\sum_{\langle ij,kl\rangle}\hat{s}^z_{ij}\hat{s}^z_{kl} - h\sum_{\langle ij\rangle}\hat{s}^x_{ij}, \quad \hat{H}_\mathrm{fs} = \sum_{\langle ij\rangle,\sigma} t_{ij}\xi_{ij}\hat{s}^z_{ij}\hat{c}^\dagger_{i\sigma}\hat{c}_{j\sigma}. \tag{7}$$

While $\hat{H}_\mathrm{f}$ corresponds to the half-filled Hubbard model on the π-flux square lattice, $\hat{H}_\mathrm{s}$ is a ferromagnetic, transverse-field Ising model defined on the bonds $\langle ij\rangle$ of the square lattice. $\hat{H}_\mathrm{fs}$ accounts for the coupling between Dirac fermions and Ising spins. The Hubbard interaction and the fermion-spin coupling can dynamically generate SO(3) AFM order and Z_2 KVBS order (ferromagnetic order of the Ising spins), respectively. For the numerical simulations, we used the ALF (ALGORITHMS FOR LATTICE FERMIONS) implementation [23] of the finite-temperature auxiliary-field QMC method [24,25]. Our model can be simulated without encountering the negative-sign problem. Henceforth, we use $t = 1$ as the energy unit, and set $J = -1$, $\xi = 0.5$, and $U = 7$. An inverse temperature $\beta = 30$ (with Trotter discretization $\Delta\tau = 0.1$) yields results representative of the ground state. QMC results on torus geometries detailed in the SM [14] suggest a continuous AFM-Z_2 KVBS transition with an emergent SO(4) symmetry at $1/h_c \approx 0.270$.

To pin a domain-wall configuration, we consider a cylindrical geometry and freeze the Ising spins at the edges to $\hat{s}^z_{(i_1,-n),(i_1,-n+1)} = 1$ and $\hat{s}^z_{(i_1,n-1),(i_1,n)} = -1$, where $L_2 = 2n+1$. Taking into account the gauge freedom to define the

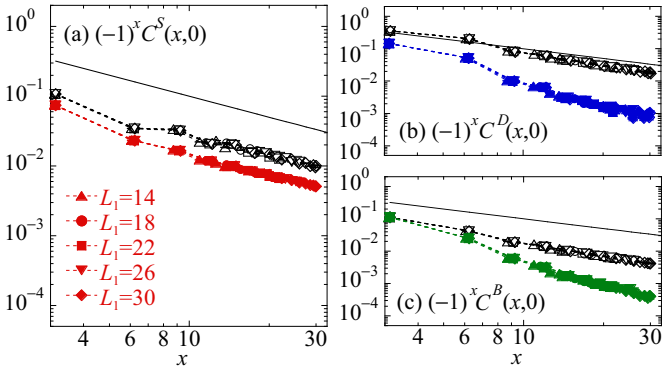

FIG. 2. Real-space correlation functions for (a) spin, (b) dimer, and (c) bond at the domain wall of Z_2 KVBS (solid symbols). Here, $L_2 = 17$ and $x = L_1 \sin(\pi i_1/L_1)$ is the conformal distance [31]. Open symbols indicate QMC results for the one-dimensional Hubbard model at $U/t = 4$ and at half filling. The solid line corresponds to x^{-1}.

π-flux model, translation symmetry by $\boldsymbol{a}_1$ is present. The model with pinning fields has a mirror symmetry corresponding to the combined transformations $\hat{c}^\dagger_{(i_1,i_2),\sigma} \to \hat{c}^\dagger_{(i_1,-i_2),\sigma}$ and $\hat{s}^z_{(i_1,i_2),(i_1,i_2+1)} \to -\hat{s}^z_{(i_1,i_2),(i_1,-i_2-1)}$.

Numerical results. To detect the profile of the domain wall, we measure the bond kinetic energy $\Delta\hat{B}_{\boldsymbol{i},\boldsymbol{a}_l} = \langle \hat{B}_{\boldsymbol{i},\boldsymbol{a}_l}\rangle - \langle \bar{B}\rangle$. Here, $\hat{B}_{\boldsymbol{i},\boldsymbol{a}_l} = \sum_\sigma t_{\boldsymbol{i},\boldsymbol{i}+\boldsymbol{a}_l}(\hat{c}^\dagger_{\boldsymbol{i}\sigma}\hat{c}_{\boldsymbol{i}+\boldsymbol{a}_l\sigma} + \hat{c}^\dagger_{\boldsymbol{i}+\boldsymbol{a}_l\sigma}\hat{c}_{\boldsymbol{i}\sigma})$ and $\bar{B} = (2L_1L_2)^{-1}\sum_{\boldsymbol{i},l}\hat{B}_{\boldsymbol{i},\boldsymbol{a}_l}$, where $l = 1, 2$. Figure 1(c) shows this quantity. The aforementioned translation and mirror symmetries are readily seen.

As discussed above, the field theory of the domain wall is described by an SO(3) nonlinear sigma model with the θ term at $\theta = \pi$ in $(1+1)$ dimensions. We expect this theory to have an emergent SO(4) [26,27] symmetry reflecting the fact that spin-spin and dimer-dimer correlations decay with the same power law but with different logarithmic corrections: $(-1)^r(\ln r)^{1/2}r^{-1}$ for the spin [28–30] and $(-1)^r(\ln r)^{-3/2}r^{-1}$ for the dimer [30]. In Figs. 2(a)–2(c), we plot the spin $[C^S(\boldsymbol{i}) = \langle \hat{\boldsymbol{S}}_{\boldsymbol{i}} \cdot \hat{\boldsymbol{S}}_{\boldsymbol{0}}\rangle]$, dimer $[C^D(\boldsymbol{i}) = \langle(\hat{\boldsymbol{D}}_{\boldsymbol{i}} - \langle\hat{\boldsymbol{D}}_{\boldsymbol{i}}\rangle)\cdot(\hat{\boldsymbol{D}}_{\boldsymbol{0}} - \langle\hat{\boldsymbol{D}}_{\boldsymbol{0}}\rangle)\rangle]$, and bond $[C^B(\boldsymbol{i}) = \langle(\hat{B}_{\boldsymbol{i},\boldsymbol{a}_1} - \langle\hat{B}_{\boldsymbol{i},\boldsymbol{a}_1}\rangle)\cdot(\hat{B}_{\boldsymbol{0},\boldsymbol{a}_1} - \langle\hat{B}_{\boldsymbol{0},\boldsymbol{a}_1}\rangle)\rangle]$ correlators as a function of the conformal distance $x = L_1\sin(\pi i_1/L_1)$ [31]. Here, $\hat{\boldsymbol{S}}_{\boldsymbol{i}} = \sum_{\sigma\sigma'}\hat{c}^\dagger_{\boldsymbol{i}\sigma}\boldsymbol{\sigma}_{\sigma\sigma'}\hat{c}_{\boldsymbol{i}\sigma'}$ and $\hat{\boldsymbol{D}}_{\boldsymbol{i}} = \hat{\boldsymbol{S}}_{\boldsymbol{i}}\cdot\hat{\boldsymbol{S}}_{\boldsymbol{i}+\boldsymbol{a}_1}$. The bond and dimer correlations share the same symmetries so that we expect them to decay with the same power law. We compare our results with those for the half-filled Hubbard chain at $U/t = 4$. While there is remarkable agreement between the spin correlations [see Fig. 2(a)], it appears that we have to reach longer length scales in the domain-wall calculation to observe the $1/r$ power-law decay for the dimer and bond correlations [see Figs. 2(b) and 2(c)]. A possible interpretation of these numerical results is that the Hubbard model is *closer* to the emergent SO(4) conformal field theory than the domain wall SO(3) theory of Eq. (5). Further evidence for the emergent spin-1/2 chain can be obtained from the dynamical spin structure factor at the domain wall that shows a two-spinon continuum (see SM [14]).

The field-theory interpretation of the domain wall has consequences. It should be independent of the choice of the lattice discretization—provided that it does not break relevant symmetries such as translation along the domain wall—and the lattice constant should correspond to a high-energy scale. In the Z_2 KVBS phase close to the critical point [Figs. 3(c) and 3(d)], we check that the domain wall extends over many lattice sites in the perpendicular direction. In particular, for the value of transverse field h considered, the domain wall extends over several lattice spacings and the data are consistent with $C^S(x, i_2) \sim e^{-|i_2|/\xi}x^{-1}$, where $\xi \sim 4$. The profile of the domain wall is expected to be inversely proportional to the stiffness. Varying $1/h$ in the Z_2 KVBS will merely change the profile of the domain wall, thereby changing the length scale ξ but not the properties of the spin-1/2 chain along the domain wall [see Figs. 3(a) and 3(b)].

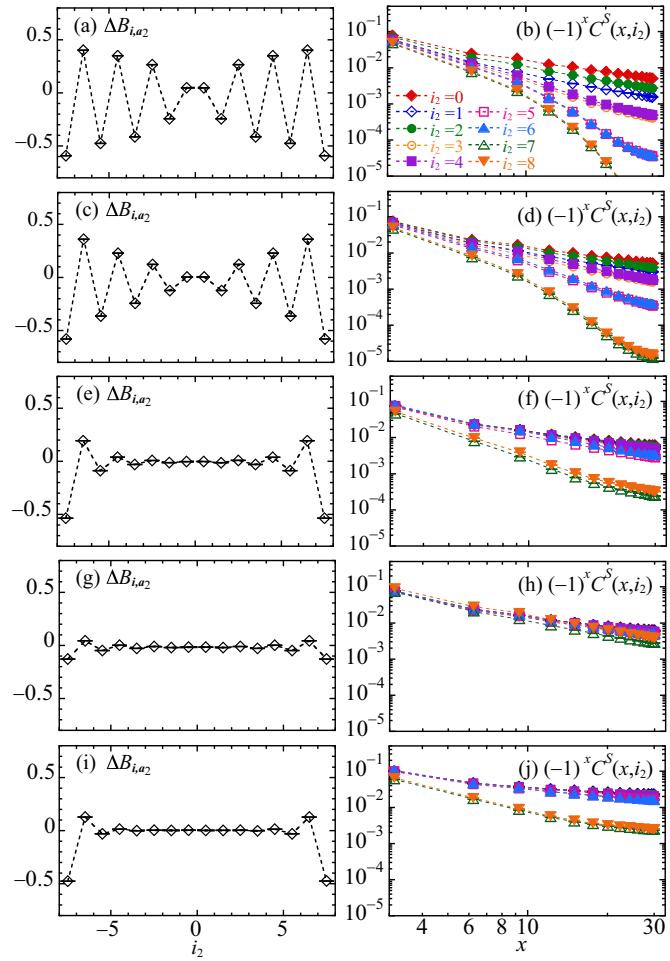

FIG. 3. Real-space bond energy change at $\boldsymbol{i} = (i_1 = 0, i_2)$ (left panels) and spin-spin correlation functions along the domain wall of Z_2 KVBS (right panels) for $L_2 = 17$ and $x = L_1\sin(\pi i_1/L_1)$ with $L_1 = 30$. (a), (b) $1/h = 0.333$ (Z_2 KVBS phase) and (c), (d) $1/h = 0.275$ (Z_2 KVBS phase close to the critical point) at $U = 7$. At $h = \infty$, our model maps onto the pure Hubbard model on the π-flux lattice and $U > 5.71(1)$ [32] places us in the AFM phase. In (e), (f) [(g), (h)], we consider this limit with [without] pinning fields at $U = 7$, and in (i), (j), the same limit with pinning fields at $U = 12$.

In contrast, in the AFM phase, there is no scale that confines the width of the domain wall other than the width of the lattice L_2. We expect the spin-spin correlations within the domain wall to show the long-range AFM order. At $h = \infty$,

our model maps onto the pure Hubbard model on the π-flux lattice and we can choose to impose or not impose pinning fields on the edge. The Gross-Neveu transition in this model occurs at $U_c = 5.71(1)$ [32] so that the value $U = 7$ underlying Figs. 3(e)–3(h) places us *far* from the critical point. As is apparent from the data, the profile of the domain wall is flat around the center of the cylinder. Although the spin correlations [see Fig. 3(f)] show a slight upturn, they do not provide clear evidence of long-range order. This counterintuitive result—on a rather large lattice—can be understood by thinking in terms of proximity to the deconfined quantum critical point (DQCP). The AFM state originates from the binding of spinons and this will occur on a confinement length scale. If L_2 is comparable to this length scale, spinons persist within the domain wall. Enhancing the interaction to $U = 12$ [see Figs. 3(i) and 3(j)] takes us away from the DQCP so that the confining spinon length scale becomes smaller. In this case, the profile of the domain wall is again very flat and spin correlations develop clear signs of ordering. It is also interesting to note that the data for $U = 7$ without pinning fields also show very anomalous spin-spin correlations [see Figs. 3(g) and 3(h)]. Thus, open boundary conditions effectively generate a KVBS mass along the edge.

Summary and discussion. We have shown how to probe topological terms in lattice realizations of field theories by pinning defects. The explicit example provided in this work is based on a model where the effective field theory has a θ term at $\theta = \pi$ in $(2+1)$ dimensions with emergent SO(4) symmetry. In the lattice realization of this model, the SO(4) symmetry reduces to SO(3)$\times$ Z_2 and we consider a domain wall of the Z_2 field. The emergent SO(4) symmetry then suggests that the domain wall harbors a spin-1/2 chain. Our numerical results not only confirm this point of view but show that topology is important to understand aspects of the physics of the Hubbard model on the π-flux lattice. We note that similar calculations have been carried out in the realm of the JQ model [33] with emphasis placed only on defects in the VBS phase. Furthermore, in Ref. [33], the pinning of the domain wall is imposed by breaking the symmetry of the bulk Hamiltonian, thus potentially changing the nature of the transition. In contrast, the pinning carried out here involves only boundary conditions.

The above argument holds for continuous transitions with emergent symmetries. There is an ongoing debate on the nature of the generic DQCP [9,34–36] with an emergent SO(5) symmetry [37]. Compelling evidence for a continuous transition with an emergent SO(5) symmetry has been put forward but critical exponents stand at odds with bootstrap bounds [38]. To resolve this apparent contradiction, one can conjecture [39–41] that an SO(5) conformal field theory indeed exists in spatial dimensions slightly greater than two that, however, collides with another fixed point and becomes complex upon tuning the dimension down to two. Proximity to fixed-point collision is at the origin of a very slow renormalization group flow and associated very long correlation lengths [39,42]. In fact, recent simulations of the SO(5) nonlinear sigma model with a WZW topological term support this point of view [43]. Very similar arguments can be applied to the present case where weakly first-order transitions were reported for similar symmetry classes [44–46]. Hence, a weakly first-order transition does not impair the notion that topological terms can play a dominant role at intermediate length scales.

Our approach allows for simulations of models previously inaccessible to Monte Carlo simulations. In two spatial dimensions, negative-sign-free QMC simulations of the SO(5) nonlinear sigma model with WZW geometrical term are possible [8,43]. As shown in the SM [14], at a domain wall generated by pinning one component of the SO(5) vector, a $(1+1)$-dimensional SO(4) nonlinear sigma model with a WZW term emerges. This model is known to capture the low-energy physics of the Heisenberg chain [26,27].

Our observation may equally have some utility in three dimensions, where there are also pairs of ordered phases for which the disorder operators for one phase are charged under the symmetry broken by the other. A simple example involves a cubic-lattice AFM and a cubic-lattice VBS [47]. As in two dimensions, the skyrmions carry lattice-symmetry quantum numbers, and the defects of the VBS pattern (which are hedgehogs) carry spin. This can be encoded in a sigma model with a WZW term, now with softly broken SO(6) $\supset$ $\mathrm{SO(3)_{AFM}} \times \mathrm{SO(3)_{VBS}}$ symmetry. However, in addition to the usual possibility of a first-order transition [48], a direct transition between these two phases can also be preempted by an intermediate disordered *phase* for the following reason: in contrast to two dimensions, compact Abelian gauge theory with small amounts of charged matter (QED) has a (familiar) deconfined phase in three dimensions. But, as in the above discussion, the WZW term still has consequences *within* the ordered phases. For definiteness and similarity with our example above, consider breaking the cubic lattice symmetry down to $Z_2 \times Z_2$, where the second Z_2 represents reflections in $\hat{z}$, say. The associated sigma model then has $\mathrm{SO(5)} \supset \mathrm{SO(3)_{AFM}} \times (Z_2 \times Z_2)_{\mathrm{VBS}}$ symmetry with a θ term at $\theta = \pi$. In analogy to the case considered here, the domain wall of the Z_2 part of the VBS order parameter transverse to the $\hat{z}$ direction will host an SO(4) nonlinear sigma model at $\theta = \pi$, now in $(2+1)$ dimensions. This is a description of the DQCP between AFM and KVBS orders in two dimensions.

Another possibility is to break the cubic-lattice symmetry down to $C_4 \times Z_2$, where again the Z_2 represents reflections in $\hat{z}$. The associated sigma model then has $\mathrm{SO(6)} \supset \mathrm{SO(3)_{AFM}} \times [\mathrm{SO(2)} \times Z_2]_{\mathrm{VBS}}$ symmetry with a WZW term. Now, the domain wall of the Z_2 part of the VBS order parameter, transverse to the $\hat{z}$ direction, will host an SO(5) nonlinear sigma model with a WZW term, now in $(2+1)$ dimensions. This construction could provide an alternative for the Landau-level projection formulation of this theory [8,43].

Acknowledgments. We thank J. S. Hofmann, M. Oshikawa, Z. Wang, C. Xu, and Yi-Zhuang You for insightful discussions, as well as A. Sandvik for bringing Ref. [33] to our attention. We thank the Gauss Centre for Supercomputing (SuperMUC at the Leibniz Supercomputing Centre) for the generous allocation of supercomputing resources. The research has been supported by the Deutsche Forschungsgemeinschaft through Grants No. AS 120/15-1 (T.S.), No. SA 3986/1-1 (T.S.), No. AS120/14-1 (F.F.A.), the Würzburg-Dresden Cluster of Excellence on Complexity and Topology in Quantum Matter - ct.qmat (EXC 2147, Project ID No. 390858490) (F.F.A.) and SFB 170 ToCoTronics (M.H.). T.G.

is supported by the National Science Foundation under Grant No. DMR-1752417 and as an Alfred P. Sloan Research Fellow. F.F.A. and T.G. thank the BaCaTeC for partial financial support.

[1] A. Abanov and P. Wiegmann, Nucl. Phys. B **570**, 685 (2000).
[2] A. Tanaka and X. Hu, Phys. Rev. Lett. **95**, 036402 (2005).
[3] T. Senthil and M. P. A. Fisher, Phys. Rev. B **74**, 064405 (2006).
[4] J. Lee and S. Sachdev, Phys. Rev. Lett. **114**, 226801 (2015).
[5] T. Grover and T. Senthil, Phys. Rev. Lett. **100**, 156804 (2008).
[6] T. Sato, M. Hohenadler, and F. F. Assaad, Phys. Rev. Lett. **119**, 197203 (2017).
[7] Z.-X. Li, Y.-F. Jiang, S.-K. Jian, and H. Yao, Nat. Commun. **8**, 314 (2017).
[8] M. Ippoliti, R. S. K. Mong, F. F. Assaad, and M. P. Zaletel, Phys. Rev. B **98**, 235108 (2018).
[9] Y. Liu, Z. Wang, T. Sato, M. Hohenadler, C. Wang, W. Guo, and F. F. Assaad, Nat. Commun. **10**, 2658 (2019).
[10] S. Ryu, C. Mudry, C.-Y. Hou, and C. Chamon, Phys. Rev. B **80**, 205319 (2009).
[11] T. Senthil, L. Balents, S. Sachdev, A. Vishwanath, and M. P. A. Fisher, Phys. Rev. B **70**, 144407 (2004).
[12] T. Senthil, A. Vishwanath, L. Balents, S. Sachdev, and M. P. A. Fisher, Science **303**, 1490 (2004).
[13] M. Levin and T. Senthil, Phys. Rev. B **70**, 220403(R) (2004).
[14] See Supplemental Material at http://link.aps.org/supplemental/10.1103/PhysRevB.104.L161105 for a derivation of the domain-wall action, i.e., a $(1+1)$-dimensional SO(3) nonlinear sigma model with θ term at $\theta=\pi$, and how to generalize this to the Wess-Zumino-Witten geometrical term, i.e., a $(1+1)$-dimensional SO(4) nonlinear sigma model with Wess-Zumino-Witten term is realized at the domain wall of the SO(5) super vector. Also included are a review of our AFQMC simulations on the torus, further evidence for the emergent spin-1/2 Heisenberg chain from the dynamical spin structure factor at the domain wall of the Z_2 KVBS, and data demonstrating the power-law decay of the real-space spin, dimer, and bond correlation functions in the one-dimensional repulsive Hubbard model at half filling, which includes Refs. [15–20].
[15] C. Wu and S.-C. Zhang, Phys. Rev. B **71**, 155115 (2005).
[16] K. Binder, Z. Phys. B **43**, 119 (1981).
[17] S. Pujari, T. C. Lang, G. Murthy, and R. K. Kaul, Phys. Rev. Lett. **117**, 086404 (2016).
[18] I. F. Herbut, V. Juričić, and B. Roy, Phys. Rev. B **79**, 085116 (2009).
[19] B. Lake, D. A. Tennant, J.-S. Caux, T. Barthel, U. Schollwöck, S. E. Nagler, and C. D. Frost, Phys. Rev. Lett. **111**, 137205 (2013).
[20] F. F. Assaad and D. Würtz, Phys. Rev. B **44**, 2681 (1991).
[21] F. D. M. Haldane, Phys. Rev. Lett. **50**, 1153 (1983).
[22] C. Mudry, *Lecture Notes on Field Theory in Condensed Matter Physics* (World Scientific, Singapore, 2014).
[23] M. Bercx, F. Goth, J. S. Hofmann, and F. F. Assaad, SciPost Phys. **3**, 013 (2017).
[24] R. Blankenbecler, D. J. Scalapino, and R. L. Sugar, Phys. Rev. D **24**, 2278 (1981).
[25] F. Assaad and H. Evertz, in *Computational Many-Particle Physics*, Lecture Notes in Physics, edited by H. Fehske, R. Schneider, and A. Weiße (Springer, Berlin, 2008), Vol. 739, pp. 277–356.
[26] I. Affleck, Phys. Rev. Lett. **55**, 1355 (1985).
[27] I. Affleck and F. D. M. Haldane, Phys. Rev. B **36**, 5291 (1987).
[28] I. Affleck, D. Gepner, H. J. Schulz, and T. Ziman, J. Phys. A: Math. Gen. **22**, 511 (1989).
[29] R. R. P. Singh, M. E. Fisher, and R. Shankar, Phys. Rev. B **39**, 2562 (1989).
[30] T. Giamarchi and H. J. Schulz, Phys. Rev. B **39**, 4620 (1989).
[31] J. Cardy, *Scaling and Renormalization in Statistical Physics* (Cambridge University Press, Cambridge, 1996).
[32] F. Parisen Toldin, M. Hohenadler, F. F. Assaad, and I. F. Herbut, Phys. Rev. B **91**, 165108 (2015).
[33] T. Sulejmanpasic, H. Shao, A. W. Sandvik, and M. Ünsal, Phys. Rev. Lett. **119**, 091601 (2017).
[34] H. Shao, W. Guo, and A. W. Sandvik, Science **352**, 213 (2016).
[35] A. Nahum, J. T. Chalker, P. Serna, M. Ortuño, and A. M. Somoza, Phys. Rev. X **5**, 041048 (2015).
[36] A. W. Sandvik and B. Zhao, Chin. Phys. Lett. **37**, 057502 (2020).
[37] A. Nahum, P. Serna, J. T. Chalker, M. Ortuño, and A. M. Somoza, Phys. Rev. Lett. **115**, 267203 (2015).
[38] D. Poland, S. Rychkov, and A. Vichi, Rev. Mod. Phys. **91**, 015002 (2019).
[39] C. Wang, A. Nahum, M. A. Metlitski, C. Xu, and T. Senthil, Phys. Rev. X **7**, 031051 (2017).
[40] A. Nahum, Phys. Rev. B **102**, 201116(R) (2020).
[41] R. Ma and C. Wang, Phys. Rev. B **102**, 020407 (2020).
[42] I. F. Herbut and L. Janssen, Phys. Rev. Lett. **113**, 106401 (2014).
[43] Z. Wang, M. P. Zaletel, R. S. K. Mong, and F. F. Assaad, Phys. Rev. Lett. **126**, 045701 (2021).
[44] E. Torres, L. Weber, L. Janssen, S. Wessel, and M. M. Scherer, Phys. Rev. Res. **2**, 022005 (2020).
[45] P. Serna and A. Nahum, Phys. Rev. B **99**, 195110 (2019).
[46] B. Zhao, P. Weinberg, and A. W. Sandvik, Nat. Phys. **15**, 678 (2019).
[47] P. Hosur, S. Ryu, and A. Vishwanath, Phys. Rev. B **81**, 045120 (2010).
[48] M. S. Block and R. K. Kaul, Phys. Rev. B **86**, 134408 (2012).